# Optimal Motions of a Welding Robot for Cooperative Tasks with a 2 DOF Positioner

Oscar I. Santellano J., J. Alfonso Pámanes G., Julio C. Rodríguez C., J. Jesús Pámanes G.

*2021 XXIII Robotics Mexican Congress (ComRob)*, Tijuana, Baja California, México, pp. 145–151, 2021.

DOI: 10.1109/ComRob53312.2021.9628721

# Optimal Motions of a Welding Robot for Cooperative Tasks with a 2 DOF Positioner

*Oscar I. Santellano J.* [1], *J. Alfonso Pámanes G.* [2], *Julio C. Rodríguez C.* [3], *J. Jesús Pámanes G.* [4]

[1 2 3 4]Division of Postgraduate Studies and Research, Tecnológico Nacional de México - Instituto Tecnológico de la Laguna
Blvd. Revolución y Calz. Cuauhtémoc Torreón, Coah, Mexico C.P. 27000
Email: [1]oscar.santellano@hotmail.com, [2]japamanesg@correo.itlalaguna.edu.mx,
[3]rodriguezcervantesjc@gmail.com, [4]jdejpamanesg@correo.itlalaguna.edu.mx

***Abstract*— The application of cooperative positioner devices for industrial robotic workstations is becoming an interesting alternative. Such devices ease the accessibility of robots to tasks and increase their productivity. Thus, motion planning of robots working in cooperation with positioners becomes a noteworthy issue for corporations. Indeed, simultaneous and continuous motions of both the positioner and the robot should be suitably designed to increase the performance of the manufacturing system. In this paper, the simultaneous motions of a robot and a positioner table are synthesized such that a complex 3D welding seam is applied on a workpiece. The degree of freedom (DOF) of the considered robot and the cooperating table are 6 and 2, respectively. The applied strategy to obtain the joint trajectories of the system allows optimizing the kinematic performance of the robot during the execution of the task. Two indices of performance of robots are optimized: the translational and the rotational manipulabilities.**

## I. Introducción

Nowadays, more and more corporations of the metal-mechanical industry are coming to apply auxiliary positioner devices (or cooperating tables) in their robotic workstations. Such devices provide easier access to complex zones of the workpieces of the robots. Additionally, the kinematic performance and the productivity of these machines could be notably improved. The motion planning of robots with cooperating tables has been studied under different approaches and distinct levels of complexity since a few years ago [2]. It can be considered, for instance, that the positioner possesses a single degree of freedom (DOF) v.gr. [2], or that the workpiece is moved by another 6-DOF robot [6]. It can be also assumed that both the robot and the positioner device move simultaneously [4] or sequentially [3].

In this paper, the development of a method for motion planning of a 6-DOF robotic manipulator is proposed for achieving tasks with the assistance of a 2-DOF positioner device. It is considered that motions of both machines are executed simultaneously. The motions are planned in such a way that the kinematic performance of the manipulator is optimized while the task is completed. The method is validated by applying it to describe a 3D path with a specified orientation of the end-effector.

In the next section, the architecture of the system is described and the basic equations to solve the kinematic modelling are presented. A brief review of the kinematic performances indices to be optimized of the manipulator is given in Section III. Then, the formulation to solve the motion planning problem is developed in Section IV. The final considerations about the proposed approach are presented in Section V.

## II. Kinematics Modelling

The welding robot-positioner system considered is composed by a Robot *Fanuc ARC Mate 100iC* and a rotational positioner *T Solda 100Kg*. This system is installed at the Laboratory of Mechatronics and Control (LaMyC) of the Tecnologico Nacional de México - Instituto Tecnologico de la Laguna (TecNM - ITLag).

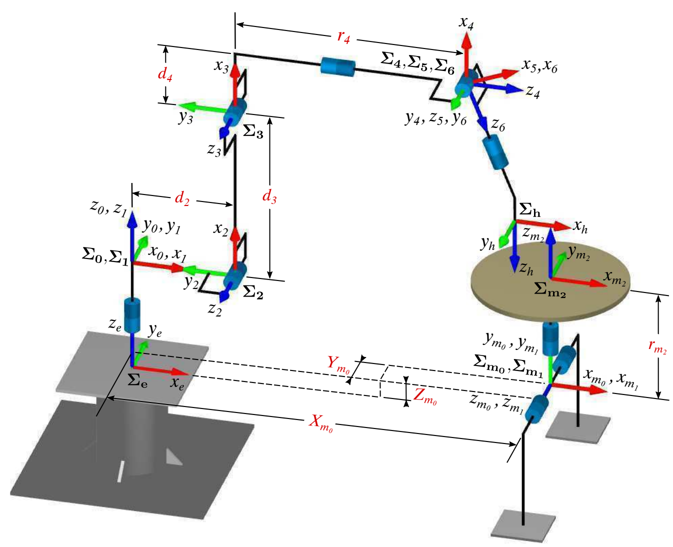


Fig. 1: The kinematic scheme of the robot–positioner system

The kinematic scheme of the system is illustrated in Figure 1, $\Sigma_e$ denotes the coordinate frame attached to the workstation and $\Sigma_0$ designates the coordinate frame attached to the base of the robot, $\Sigma_1$, $\Sigma_2, \cdots, \Sigma_6$ represents the coordinate frames attached to the successive mobile links of the robot (from the shoulder to the end-effector), respectively. $\Sigma_h$ designates the coordinate frame attached to the welding torch, with the origin at the tip of the tool. $\Sigma_{m_0}$ denotates the coordinate frame attached to the base of the positioner table. $\Sigma_{m_1}$ and $\Sigma_{m_2}$ represent the coordinate frames attached to the mobile links 1 and 2 (platform) of the positioner, respectively. All of frames of the manipulator are defined based on the modified Denavit-Hartenberg (D-H) notation [7].

The modified D-H parameters for the kinematic chain of the robot are displayed in Table I. The corresponding parameters of the positioner table are given in Table II.

TABLE I: MODIFIED DENAVIT-HARTENBERG PARAMETERS OF THE *FANUC ROBOT ARC MATE® 100/IC*.

| $j$ | $\sigma_j$ | $\alpha_j(°)$ | $d_j$ | $\theta_j$ | $r_j$ |
|---|---|---|---|---|---|
| *1* | 0 | 0 | 0 | $\theta_1$ | 0 |
| *2* | 0 | 90 | $d_2$ | $\theta_2$ | 0 |
| *3* | 0 | 0 | $d_3$ | $\theta_3$ | 0 |
| *4* | 0 | 90 | $d_4$ | $\theta_4$ | $r_4$ |
| *5* | 0 | $-90$ | 0 | $\theta_5$ | 0 |
| *6* | 0 | 90 | 0 | $\theta_6$ | 0 |

$d_2 = 150\ mm$; $d_3 = 600\ mm$; $d_4 = 200\ mm$; $r_4 = 640\ mm$

TABLE II: MODIFIED DENAVIT-HARTENBERG PARAMETERS OF THE *T SOLDA®* POSITIONER.

| $j$ | $\sigma_{m_j}$ | $\alpha_{m_j}(°)$ | $d_{m_j}$ | $\phi_j$ | $r_{m_j}$ |
|---|---|---|---|---|---|
| *1* | 0 | 0 | 0 | $\phi_1$ | 0 |
| 2 | 0 | $-90$ | 0 | $\phi_2$ | $r_{m2}$ |

$r_{m_2} = 130\ mm$

From the geometric parameters and employing the SYMORO (SYmbolic MOdeling of RObots) software [8], the kinematic models of the robot and the positioner are obtained. The inverse kinematic model is applied in the formulation to determine the joint variables corresponding to the desired task, with simultaneous motions of the positioner that optimize the kinematic performance of the manipulator. The Jacobian matrix of the robot is considered to evaluate the kinematic performance of the manipulator by using the manipulability indices.

The tool frame $\Sigma_h$ shown in Figure 2 , allows to specify the desired motion of the welding torch. The pose of the frame $\Sigma_h$ with respect to $\Sigma_6$ is defined by the matrix (1):

$$ {}^6_hT = \begin{bmatrix} \sin\rho & 0 & -\sin\rho & d_{hx} \\ 0 & 1 & 0 & d_{hy} \\ \cos\rho & 0 & \cos\rho & d_{hz} \\ 0 & 0 & 0 & 1 \end{bmatrix} \tag{1} $$

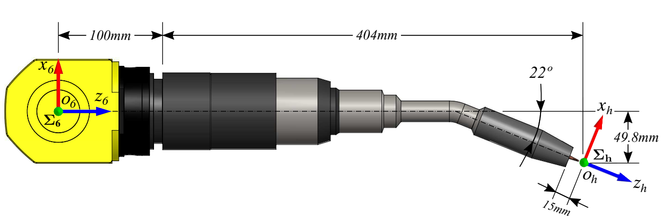


Fig. 2: Torch *ABIROB A500 22* of the robot *Fanuc 100iC/12*.

where $\rho = -22°$, $d_{hx} = -49.8\ mm$, $d_{hy} = 0\ mm$ and $d_{hz} = 504\ mm$.

The homogeneous transformation matrix that specifies the robot location into the workstation, is given by:

$$ {}^e_0T = \begin{bmatrix} 1 & 0 & 0 & e_x \\ 0 & 1 & 0 & e_y \\ 0 & 0 & 1 & e_z \\ 0 & 0 & 0 & 1 \end{bmatrix} \tag{2} $$

where $e_x = 0\,mm$, $e_y = 0\,mm$ and $e_z = 450\ mm$. Similarly, the placement of the positioner table with respect to the frame $\Sigma_e$ is specified by the matrix (3):

$$ {}^e_{m_0}T = \begin{bmatrix} \cos\mu & 0 & \sin\mu & X_{m_0} \\ \sin\mu & 0 & -\cos\mu & Y_{m_0} \\ 0 & 1 & 0 & Z_{m_0} \\ 0 & 0 & 0 & 1 \end{bmatrix} \tag{3} $$

The orientation of $\Sigma_{m_0}$ with respect to $\Sigma_e$ in (3) is specified by the Bryant's angles $\lambda$, $\mu$ and $\nu$ (rotations in the order $Z$-$Y$-$Z$). The angles $\lambda$ and $\nu$ are specified, 90° and 0°, respectively, in such a way that the base frame of the table match with the plane of the floor.

On the other hand, the placement of the frame attached to the rotating platform of the positioner table, with respect to the fixed base of the table is obtained as:

$$ {}^{m_2}_{m_0}T = \begin{bmatrix} c\phi_1 c\phi_2 & -c\phi_1 s\phi_2 & -s\phi_1 & -r_{m_2} s\phi_1 \\ s\phi_1 c\phi_2 & -s\phi_1 s\phi_2 & c\phi_1 & r_{m_2} c\phi_1 \\ -s\phi_2 & c\phi_1 c\phi_2 & 0 & 0 \\ 0 & 0 & 0 & 1 \end{bmatrix} \tag{4} $$

The parameter $r_{m_2}$ in (4) is known from the architecture of the table. The variables $\mu$, $X_{m_0}$, $Y_{m_0}$ and $Z_{m_0}$ in (3), and $\phi_1$ in (4) are related with the design of the workstation. Suitable values of such variables were obtained in [14]. All these variables remain constant during the execution of the task. Its values are kept in $90°$, $1200\,mm$, $500\,mm$, $-10\,mm$ and $10.4°$, respectively. The variables $\phi_2$ in (4), and $\psi$ defining the orientation of the torch will be synthesized in Section IV, as time functions such that the manipulator's kinematic performance be optimized during the execution of the desired task.

The pose of the torch whit respect to the workstation can be obtained via both the manipulator and the positioner table. The corresponding equations are (5) and (6), respectively:

$$ {}^e_hT = {}^e_0T\ {}^0_1T\ {}^1_2T\ {}^2_3T\ {}^3_4T\ {}^4_5T\ {}^5_6T\ {}^6_hT \tag{5} $$

$$ {}^e_hT = {}^e_{m_0}T\ {}^{m_0}_{m_2}T\ {}^{m_2}_kT\ {}^k_hT \tag{6} $$

where ${}^{m_2}_kT$ is a matrix that defines the pose of the auxiliary frame $\Sigma_k$ attached to workpiece with respect to the frame $\Sigma_{m_2}$, and the matrix ${}^k_hT$ defines the desired pose of the end effector with respect to the frame $\Sigma_k$.

On the other hand, the desired pose of $\Sigma_6$ with respect to $\Sigma_0$, termed as ${}^0_6T^*$ can be found by equating (5) and (6) and solving for ${}^0_6T^*$, as folows:

$$ {}^0_6T^* = {}^e_0T^{-1}\ {}^e_{m_0}T\ {}^{m_0}_{m_2}T\ {}^{m_2}_kT\ {}^k_hT\ {}^6_hT^{-1} \tag{7} $$

Once ${}^{0}_{6}T^{*}$ is known the inverse kinematics can be explicitily solved and the corresponding posture of the manipulator is defined for a given pose of the torch.

## III. Kinematic Performance of the Manipulator

On the other hand, the twist of the end-effector of the robot is given by:

$$\boldsymbol{t} = \boldsymbol{J}(\boldsymbol{q})\dot{\boldsymbol{q}} \tag{8}$$

where the elements of the vector $\dot{\boldsymbol{q}} \in \mathbb{R}^n$ are the joint velocities of the manipulator, and $\boldsymbol{J}(\boldsymbol{q}) \in \mathbb{R}^{m\times n}$ is the basic Jacobian matrix of the manipulator [5]. The entries of such a matrix are designated as shown in (8), which can be obtained by symbolic computation using the SYMORO software.

$$\boldsymbol{J}(\boldsymbol{q}) = \begin{bmatrix} J_{11} & J_{12} & J_{13} & \cdots & J_{16} \\ J_{21} & J_{22} & J_{23} & \cdots & J_{26} \\ J_{31} & J_{32} & J_{33} & \cdots & J_{36} \\ \vdots & \vdots & \vdots & \ddots & \vdots \\ J_{61} & J_{62} & J_{63} & \cdots & J_{66} \end{bmatrix} \tag{9}$$

The twist $\boldsymbol{t}$ of the tool $\in \mathbb{R}^m$ is defined as follows:

$$\boldsymbol{t} \equiv \begin{bmatrix} \dot{\boldsymbol{p}} & \boldsymbol{\omega} \end{bmatrix}^T \tag{10}$$

In (10), $\dot{\boldsymbol{p}}$ is the velocity of the tool center point (TCP) of the end-effector, $\boldsymbol{p}$ being the position vector of such a point with respect to the frame $\Sigma_0$. The TCP considered in this study is $O_6$, shown in Figure 2. The vector $\boldsymbol{\omega}$ is the angular velocity of the end-effector. Both $\dot{\boldsymbol{p}}$ and $\boldsymbol{\omega}$ are expressed in terms of their Cartesian components with respect to the frame $\Sigma_0$.

Several kinematic performance indices have been proposed in the scientific literature, based on the Jacobian matrix of manipulators to assess their quality of motions. The *manipulability* index proposed by Yoshikawa [15] is one of the most useful indices for measuring the kinematic performance. Such an index evaluates the ease to displace the end-effector with both, translational and rotational motions. These features were considered as quite suitable for the present work. Therefore, the indices of translational and rotational manipulabilities [16] should be optimized by the manipulator during the execution of the desired task. To be able to apply such indices, we consider the Fanuc robot as composed by two kinematic sub-chains: the first one associated with the arm and the other with the wrist. The arm has $n_{\mathrm{A}} = 3$ joints and the wrist has $n_{\mathrm{W}} = 3$ joints. Thus, the translational manipulability ($w_T$) of the arm and the rotational manipulability ($w_R$) of the wrist, are respectively defined as:

$$w_T = \sqrt{\det(J_{TA}{J_{TA}}^T)} \tag{11}$$

$$w_R = \sqrt{\det(J_{RW}{J_{RW}}^T)} \tag{12}$$

where $J_{TA}$ and $J_{RW}$ are the partitions of the manipulator's basic Jacobian matrix (9), defined as:

$$J_{TA} = \begin{bmatrix} J_{11} & J_{12} & J_{13} \\ J_{21} & J_{22} & J_{23} \\ J_{31} & J_{32} & J_{33} \end{bmatrix} \tag{13}$$

$$J_{RW} = \begin{bmatrix} J_{44} & J_{45} & J_{46} \\ J_{54} & J_{55} & J_{56} \\ J_{64} & J_{65} & J_{66} \end{bmatrix} \tag{14}$$

The Rotational manipulability $w_R$ is bounded as $0 \leq w_R \leq 1$. However, the translational manipulability should be normalized in order to consistently compare the values of $w_T$ with those of $w_R$. The normalized translational manipulability is defined as:

$${w_T}^* = \frac{w_T}{w_{Tmax}} \tag{15}$$

where $w_{T_{max}}$ is the maximal translational manipulability that could obtain the manipulator with the optimal posture. In the case of the robot considered in this paper, $w_{Tmax} = 0.45\,m^3$. Thus, ${w_T}^*$ is bounded as $0 \leq {w_T}^* \leq 1$. The greater the manipulabilities are, the better the ease to obtain translational and rotational motions of the end-effector. In contrast, when any of the manipulabilities is equal zero, the manipulator gets a singular posture, and it loses the ability to produce translational or rotational motions of the end-effector on a specific direction. Moreover, in the neighborhood of a singular posture, one or both manipulabilities have small amounts and, consequently, the ability of the manipulator is quite poor to generate arbitrary displacements on specific directions.

## IV. Motion Planning

The motion planning problem considered in this Section consists in synthesizing the joint trajectories $\phi_1(t)$, $\phi_2(t)$ and $\psi(t)$ that eases the execution of the desired task to the robot. As observed in Figure 3, the former variable defines the posture of the positioner table, and the last one corresponds to one coordinate of orientation of the robot tool. By defining such trajectories, the whole postures of the robot can be computed by applying the inverse kinematic model of the robot. As indicated in Section II, a preliminary value was suitably specified for $\phi_1$ [14]. We will see that such an angle doesn't require be defined by a time function.

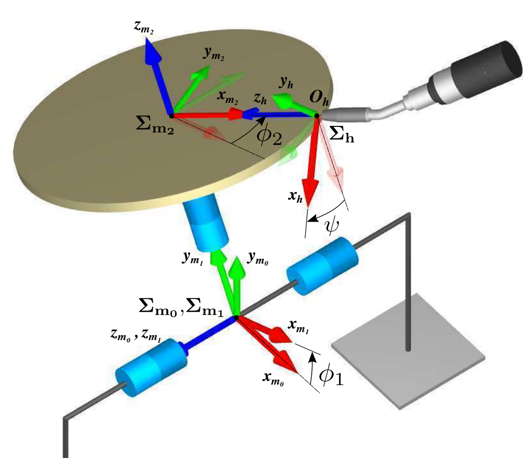

Fig. 3: Angles subject to the motion optimization process.

The synthesis should be achieved in such a way that both the translational and the rotational manipulabilities of the robot be optimized during the execution of the desired task. It must be noted that, even if the orientation of the torch should be specified considering the quality of the welding process, the coordinate $\psi$ could be defined under other criteria since the welding can be properly achieved by using any value of such an angle because of the symmetry of the tool tip.

To present the approach proposed in this paper, a task is considered in our formulation such that the robot has to apply a welding seam on the external surface of a cylinder in a time $T$ of 40 seconds at a constant speed. The geometry of the welding seam is defined by a one cycle helical curve with a radius $r_t$ of 100 $mm$ and a height $h_t$ of 450 $mm$. This path is shown in Figure 4. The longitudinal axis of the helical path matches the $z$ axis of the frame $\Sigma_k$ attached to the base of the cylinder, as shown in Figure 4.

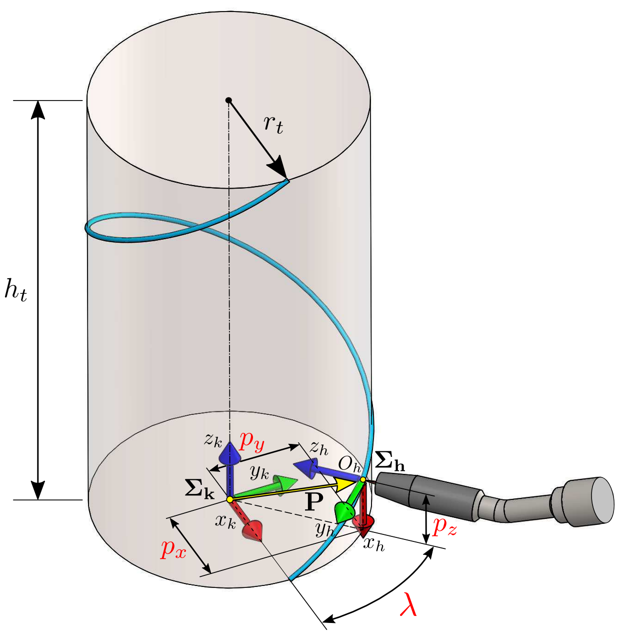

Fig. 4: Desired tool path and orientation for the welding task.

The desired position of the origin $O_h$ with respect to $\Sigma_k$ is defined by the position vector defined in (16), whose Cartesian components are given by the time functions (17):

$$\boldsymbol{P} = \begin{bmatrix} p_x(t) & p_y(t) & p_z(t) \end{bmatrix}^T \tag{16}$$

where,

$$p_x(t) = r_t \cos(\lambda(t)) \tag{17a}$$
$$p_y(t) = r_t \sin(\lambda(t)) \tag{17b}$$
$$p_z(t) = h_t \frac{t}{T} \tag{17c}$$

In (17a) $\lambda(t)$ is the angle between the $x_k$ axis and the projection of $\boldsymbol{P}$ in the $x_k$ - $y_k$ plane, as observed in Figure 4. The time function that defines this angle is expressed as:

$$\lambda(t) = 2\pi t/T \tag{18}$$

The orientation of the end-effector is specified by the Euler angles $\phi$, $\theta$ and $\psi$ (in $Z$-$Y$-$Z$ order) of the frame $\Sigma_h$, with respect to $\Sigma_k$. These coordinates are specified as follows:

$$\phi(t) = 180° + \lambda(t) \tag{19}$$
$$\theta = 90° \tag{20}$$
$$\psi(t) = \psi(t) \tag{21}$$

where, (19) keep the tip of the torch normal to the external surface of the cylinder curve with radius $r_t$. $\psi(t)$ is a time function to be proposed in the optimization process. This angle take values from 180° to −180°.

The homogeneous matrix that specifies the pose of the torch at each point of the path is:

$$^k_hT = \begin{bmatrix} ^k_h\boldsymbol{R} & \boldsymbol{P} \\ \boldsymbol{0}^T & 1 \end{bmatrix} \tag{22}$$

where the rotation matrix $^k_h\boldsymbol{R}$ is given by

$$^k_h\boldsymbol{R} = \begin{bmatrix} c\phi c\theta c\psi - s\phi s\psi & -c\phi c\theta s\psi - s\phi c\psi & c\phi s\theta \\ s\phi c\theta c\psi + c\phi s\psi & -s\phi c\theta s\psi + c\phi c\psi & s\phi s\theta \\ -s\theta c\psi & s\theta s\psi & c\theta \end{bmatrix} \tag{23}$$

where $c\bullet \equiv \cos\bullet$ and $s\bullet \equiv \sin\bullet$.

The objective function to be minimized in the optimization process is the one defined in [11] as:

$$f = -(\overline{w} - w_\sigma) \tag{24}$$

where $\overline{w}$ is the mean of the mixed manipulabilities corresponding to a sample of $n_p$ points of the desired path of the end-effector. And $w_\sigma$ is the standard deviation of the same sample. Thus, the difference $\overline{w} - w_\sigma$ represents a typically small *mixed manipulability* in the set of the mixed manipulabilities of the sample. Consequently, by minimizing the function (24), we globally maximize the whole set of mixed manipulabilities corresponding to the task.

The mixed manipulability associated with the *i*-th path point $(i = 1, 2, \cdots, n_p)$ is defined as:

$$w_i \equiv \overline{w_i{}^*} - w^*{}_{\sigma i} \tag{25}$$

where $\overline{w_i{}^*}$ is the mean of the normalized translational manipulability ($w^*{}_{Ti}$) and the rotational manipulability ($w_{Ri}$) corresponding to the posture of the manipulator at the *i*-th path point. Besides, $w^*{}_{\sigma i}$ is the standard deviation of both manipulabilities at the same point. Therefore, the mixed manipulability represents a typically small manipulability (among $w^*{}_{Ti}$ and $w_{Ri}$) of the robot at the *i*-th path point.

On the other hand, because of the welding seam must be applied on a cylindrical surface, the joint variable $\phi_2$ could be employed to rotate, about its own axis, the cylinder to be welded. As a result, the robot couldn't require moving the torch around the cylinder. Only motions of the torch in the neighborhood of a plane should be necessaries to describe the helicoidal path and to keep the desired orientation of the tool. Thus, the time function considered for the joint variable $\phi_2$ will be defined such that its first derivative be constant, with semi-cycloidal motions for starting and stopping motion. We propose:

$$\phi_2(t) = \begin{cases} \phi_2(t_0)+\Delta_1\left[\dfrac{t-t_0}{T_1}-\dfrac{\sin\left(\frac{\pi(t-t_0)}{T_1}\right)}{\pi}\right] & , \quad t_0 \le t \le t_1 \\ \phi_2(t_1)+\dfrac{\Delta_2}{T_2}(t-t_1) & , \quad t_1 \le t \le t_2 \\ \phi_2(t_2)+\Delta_3\left[\dfrac{t-t_2}{T_3}+\dfrac{\sin\left(\frac{\pi(t-t_2)}{T_3}\right)}{\pi}\right] & , \quad t_2 \le t \le T \end{cases} \tag{26}$$

$$\dot{\phi}_2(t) = \begin{cases} \dfrac{\Delta_1}{T_1}\left[1-\cos\left(\frac{\pi(t-t_0)}{T_1}\right)\right] & , \quad t_0 \le t \le t_1 \\ \dfrac{\Delta_2}{T_2} & , \quad t_1 \le t \le t_2 \\ \dfrac{\Delta_3}{T_3}\left[1+\cos\left(\frac{\pi(t-t_2)}{T_3}\right)\right] & , \quad t_2 \le t \le T \end{cases} \tag{27}$$

where the parameters of these equations are shown in the Table III.

TABLE III: PARAMETERS OF THE EQUATIONS (26) AND (27).

| $i$ | $t_{i-1}$ | $T_i$ | $\phi_2(t_{i-1})$ | $\Delta_i$ |
|---|---|---|---|---|
| 1 | $0\ s$ | $2.5\ s$ | $180^\circ$ | $-12^\circ$ |
| 2 | $2.5\ s$ | $35\ s$ | $168^\circ$ | $-336^\circ$ |
| 3 | $37.5\ s$ | $2.5\ s$ | $-168^\circ$ | $-12^\circ$ |

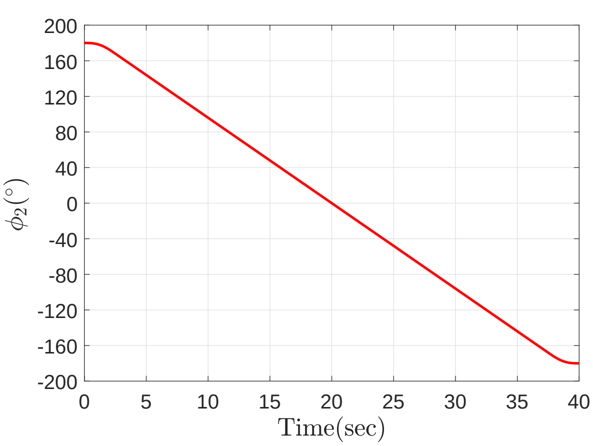


Fig. 5: Synthesized time function for $\phi_2(t)$.

Once the time function of $\phi_2$ has been defined, an exploration is carried out in order to identify a time function for the variable $\psi$ associated with the orientation of the tool. Our analysis is based on the use of performance maps [13]. In the problem considered here, an interesting performance map allow to observe the zones in the plane defined by the variables $t$ and $\psi$ that provide the postures corresponding to the desired task that give the better mixed manipulabilities of the robot. In Figure 6 it may be observed this performance map. The top view of the map is displayed in Figure 7. In this projection it is possible to visualize a continuous path for $\psi$, that goes from

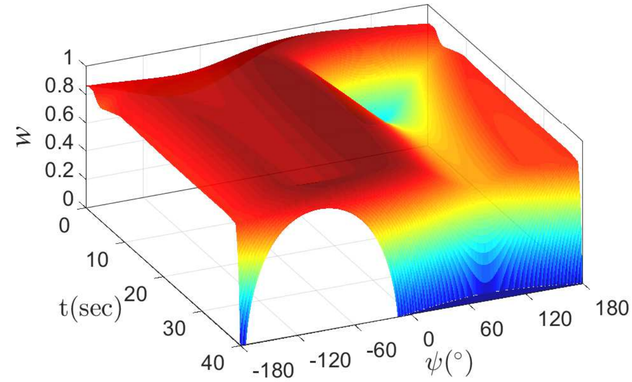


Fig. 6: Performance map of the robot *Fanuc 100iC/12*.

$t_0 = 0$ until $T = 40$ seconds, such that higher values of $w$ may be obtained. To synthesize a continuous path on this map, five via points are strategically selected, which give higher values of $w$ along the path. These points are then jointed by using cycloidal functions in such a way that continuous and smooth motions of the tool be gotten. As a result, the curve in black color is obtained. This curve is composed by four cycloidal functions ($n_f = 4$), that may be represented by (28).

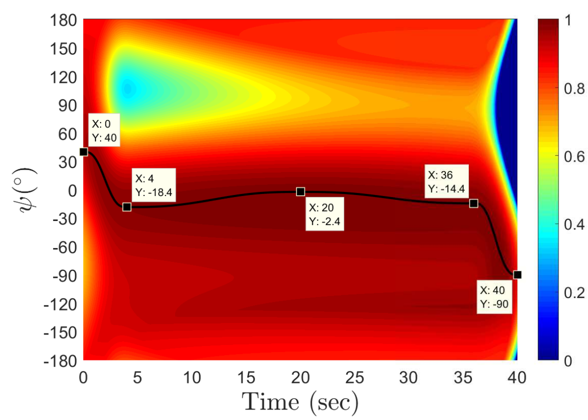


Fig. 7: Contour lines of the robot performance map for the desired task, and synthesized optimal trajectory for the angle $\psi$.

$$\psi_i(t) = \psi(t_{i-1})+\delta\psi_i\left[\frac{t-t_{i-i}}{T_i}-\frac{1}{2\pi}\sin\left(\frac{2\pi(t-t_{i-1})}{T_i}\right)\right] \tag{28}$$

The $i$-th cycloidal function is bounded by $t_{i-1} \le t \le t_i$ where $i = \{1, 2, \cdots, n_f\}$. The corresponding parameters for each interval are given in Table IV.

Thus, by employing $\phi_1 = 10.4^\circ$, and the time functions (26) and (27) for $\phi_2(t)$, and (28) for $\psi(t)$, the matrices ${}^{m_0}_{m_2}T$, ${}^{m_2}_{k}T$ and ${}^{k}_{h}T$ may be finally specified on each time sample in the interval from 0 to $40\,s$. These matrices are applied in (7) to determine ${}^{0}_{6}T^{*}$, which is the desired *SNAP* matrix of the Paul's method to solve the inverse kinematic problem [5] on each time sample.

TABLE IV: PARAMETERS OF EQUATION (28).

| $i$ | $t_{i-1}$ | $T_i$ | $\psi(t_{i-1})$ | $\delta\psi_i$ |
|---|---|---|---|---|
| 1 | $0\,s$ | $4\,s$ | $40°$ | $-58.4°$ |
| 2 | $4\,s$ | $16\,s$ | $-18.4°$ | $16°$ |
| 3 | $20\,s$ | $16\,s$ | $-2.4°$ | $-12°$ |
| 4 | $36\,s$ | $4\,s$ | $-14.4°$ | $-76.6°$ |

The obtained joint trajectories are presented in Figure 8. They allow us to carry out an analysis of the robot's translational and rotational manipulabilities in order to assess the effectiveness of our approach. The curves in Figure 9 show the behavior of such indices of performance. It can be appreciated that both indices are basically equal to 1 on all the points along the task. Notice that it is not required to move the value of the joint variable $\phi_1$ along the time to improve the performance of the robot. Only time functions are necessary for $\phi_2$ and $\psi$.

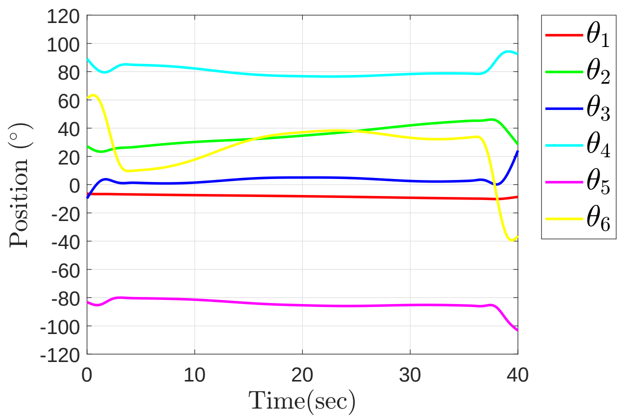


Fig. 8: Joint variables of the robot *Fanuc 100iC/12*.

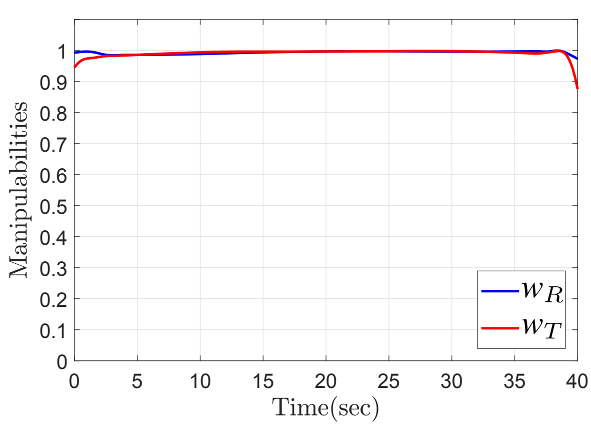


Fig. 9: Translational and rotational manipulabilities of the robot during the execution of the task.

To validate the results, the obtained joint trajectories of the robot were finally applied as control signals during an experiment in the laboratory. A sequence of postures of the robot during the experiment is displayed in Figure 10.

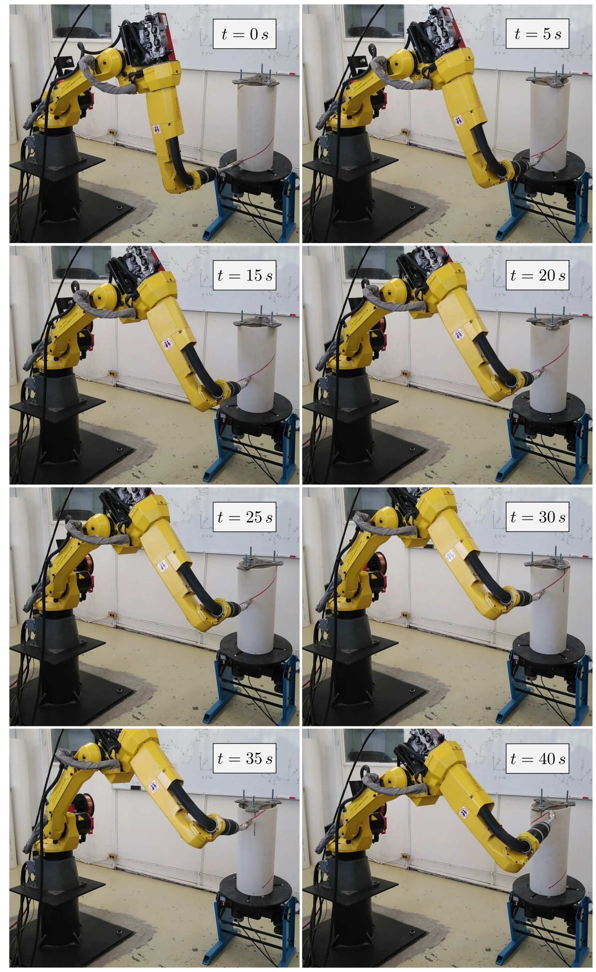


Fig. 10: Sequence of postures of the robot and the positioner table, obtained during the task execution.

## V. Conclusions

The proposed approach for motion planning of a 6-DOF robotic manipulator, working in cooperation with a 2-DOF positioner table, is effective for optimizing the kinematic performance of the robot during the task execution. The synthesized trajectories were validated by achieving experimental tests in the LaMyC of the TecNM-ITLag. The method was used to optimize the translational and rotational manipulabilities of the robot. However, other indices of performance could be optimized.

An experimental site was developed by incorporating a positioner table and its control system to the workstation of the industrial robot of the TecNM-ITLag. Thus, the LaMyC is already equipped with human and material resources of hardware and software to provide service to the industry if necessary for motion planning of cooperative robotic systems.

Even if constraints to the proposed formulation were not necessary for avoiding collisions or for preventing transgressions of joint limits while the optimization of the main criterion is being optimized, in future works such constraints should be incorporated to the method in order to enable our software tools to solve more complex problems.

## VI. Acknowledgments

The work reported in this paper was sponsored by the Tecnologico Nacional de México, the Instituto Tecnologico de la Laguna and the CONACyT of Mexico. Thanks to these agencies for their support.

## References

[1] Alatartsev S., Stellmacher S., and Ortmeier F., "*Robotic Task Sequencing Problem: A Survey*"; Journal of Intelligent and Robotic Systems, Vol. 80, Issue 2, pp. 279-298 (2015).

[2] Chen H., Liu Z., "*Offline Programming for an Arc Welding Robot with Redundant GDL*", Applied Mechanics and Materials, Vols. 184-185, pp. 1623-1627 (2012).

[3] De Anda J., "*Motion Planning of a Welding Robot for Cooperative Tasks with a Sequential Positioning Device*", XX Congreso Mexicano de Robótica (COMRob), pp. 1-6 (2018)

[4] Dena O., "*Optimal motion planning of an industrial robot operating simultaneously with a positioner table in welding tasks*", Master in Science Thesis, Tecnológico Nacional de México - Instituto Tecnológico de la Laguna (2019).

[5] Dombre E., and Khalil W., "*Modélisation et Commande des Robots*", Paris, Edition Hermes 1988.

[6] Hemmerle J.S., and Prinz F.B., "*Optimal path placement for kinematically redundant manipulators*", Proceedings of the 1991 International Conference on Robotics and Automation, pp. 1234-1243 (1991).

[7] Khalil W., and Kleinfinger J.F., "*A new geometric notation for open and closed- loop robots*", Proc. of the 1986 IEEE Conference on robotics and Automation; pp. 1174-1180 (1986).

[8] Khalil W., and Lemoine Ph., SYMORO+ Symbolic Modeling of Robots: User Guide, IRCCyN (*Institut de Recherche en Communication et Cybernétique de Nantes*), Nantes, Francia, 2003.

[9] Lin Y., Zhao H., and Ding H., "*Posture optimization methodology of 6R industrial robots for machining using performance evaluation indexes*", Robotics and Computer Integrated Manufacturing, 48, pp 59-72 (2017).

[10] Pamanes J.A., Blásquez J.R., and Llama M.A., "*Análisis de la redundancia cinemática de robots industriales en tareas de soldadura*", Memorias del XII Congreso Internacional Anual de la SOMIM (Sociedad Mexicana de Ingeniería Mecánica), pp. 571-579, (2016).

[11] Pámanes J.A., Cuán E. and Zeghloul S., "*Single and multi-objective optimization of path placement for redundant robotic manipulators*", INGENIERÍA Investigación y Tecnología, Vol. IX, No. 3, pp. 231-257; México, Jul-Sept 2008.

[12] Pámanes J.A., Soto D., Llama M.A., and Reveles D., "*Optimization of the design of an experimental robotic welding station*", Memorias del XVIII Congreso Mexicano de Robótica (COMRob), de la AMRob, pp. 179-188 (2016).

[13] Reveles D, Pámanes JA, and Wenger Ph, "*Trajectory planning of kinematically redundant parallel manipulators by using multiple working modes*", Mechanism and Machine Theory. Vol. 98, pp. 216-230, (2016).

[14] Santellano O.I., "*Motion planning of an industrial robot operating simultaneously with a 2 DOF positioner table*", Master in Science Thesis, Tecnológico Nacional de México - Instituto Tecnológico de la Laguna (2021).

[15] Yoshikawa T, "*Manipulability of Robotic Mechanisms*", International Journal of Robotics Research, Vol. 4, No. 2, pp. 3-9 (1985).

[16] Yoshikawa T, "*Translational and Rotational Manipulability of robotic Manipulators*", Proceedings of the American Control Conference, pp. 228-233 (1990).

[17] Zeghloul S., Pamanes J.A., "*Multi-criteria optimal placement of robotics in constrained environments*", Robotica, Vol. 11, pp 105-110, (1993).